Biointerface Research in Applied Chemistry
Open-Access Journal (ISSN: 2069-5837)

Article
Volume 15, Issue 1, 2025, 4
https://doi.org/10.33263/BRIAC151.004

N-[5-(4-fluorobenzyl)-1,3-thiazol-2-yl]chroman-3-Carboxamide as Antitumor Agent. Synthesis, ADME-Tox Parameters, Prediction of Metabolism Pathway and Biological Activity

Oksana Khropot [1], Iryna Drapak [1], Yuliia Matiichuk [1], Nataliia Chemerys [1], Vasyl Matiychuk [2,*]

[1] Danylo Halytsky Lviv National Medical University, Lviv, Ukraine; lvov.mp@gmail.com (O.K.); iradrapak@ukr.net (I.D.); yulm77@gmail.com (Y.M.); chemerus.talj@gmail.com (N.C.);
[2] Ivan Franko National University of Lviv, Lviv, Ukraine; v_matiychuk@ukr.net (V.M.);
* Correspondence: v_matiychuk@ukr.net;

Scopus Author ID 6506975895
Received: 18.10.2024; Accepted: 2.01.2025; Published: 12.02.2025

Abstract: It was synthesized *N*-[5-(4-fluorobenzyl)-1,3-thiazol-2-yl]chroman-3-carboxamide. The structure of the title compound was confirmed by ^{1}H NMR spectroscopy and elemental analysis. The synthesized compound complies with Lipinski, Muegge, Ghose, Veber, and Egan rules. ADME and toxicity of the compound are analyzed, and Swiss target prediction of the compound has been carried out to analyze the preferred target. The title compound exhibited remarkable anticancer activity against all the tested cell lines and was more active than classical anticancer drugs – gefitinib, 5-fluorouracil, cisplatin, and curcumin. The metabolic pathway mediated by Cytochrome P450 was evaluated for the title compound. It was found that the main pathways are aromatic hydroxylation of fused benzene ring, which should not cause toxic effects.

Keywords: thiazole; chroman; virtual screening; drug-like molecules; anticancer activity; Cytochrome P450; metabolism.

1. Introduction

Among the five-membered nitrogen-containing heterocyclic compounds, thiazole is among the most commonly used drugs. In particular, the 2-aminothiazole scaffold is considered a privileged scaffold for the discovery of anti-cancer agents based on biological targets, such as tubulin protein, histone acetylase/histone deacetylase (HAT/HDAC), phosphatidylinositol 3-kinases (PI3Ks), Src/Abl kinase, BRAF kinase, epidermal growth factor receptor (EGFR) kinase and sphingosine kinase (SphK) [1,2]. Additionally, various 2-aminothiazole-based derivatives have been used as pharmaceutical agents against different human diseases with high therapeutic effects [2].

The chromane cycle is also a structural unit of versatile, biologically attractive scaffold. It is essential to many natural compounds [3] and medicines with a simple structure and mild adverse effects [3-9]. They are also used as food additives and flavorings, in cosmetics, as optical brighteners, as laser medium in a dye laser, and as agrochemicals [10]. The most

important are 2H and 4H-chromenes – coumarins, chromen-4-ones and flavonoids. Their structures are shown in Figure 1.

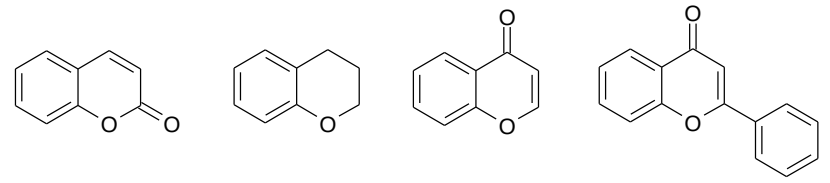

Figure 1. Structures of important chromane derivatives.

Most chromane derivatives are currently considered privileged structures in medicinal chemistry [3-9].

These facts indicate that thiazole derivatives integrated with coumarin moieties are promising to evaluate their biological activity, particularly antitumor activity [1, 11]. It also should be noted that the synthesis methods of both heterocyclic derivatives are well-developed and easy to realize [2, 10, 12].

2. Materials and Methods

2.1. Materials.

All reagents and solvents were purchased from Sigma Aldrich Chemicals and were used without further purification.

2.2. Chemistry.

The melting point was determined in an open capillary and was uncorrected. Elemental analysis was performed on a vario MICRO cube automatic CHN analyzer. The ^{1}H NMR spectra were recorded using Varian Mercury 400 (400 MHz) at 298 K. Chemical shifts were reported as δ, ppm relative to tetramethylsilane (TMS) as an internal standard. The coupling constant *J* was expressed in Hz.

2.2.1. Synthesis of chroman-3-carboxylic acid **4**.

2.04 g (0.01 mol) of ester **3** and 0.5 g of NaOH were dissolved in 50 mL of a water-alcohol mixture1:1. The reaction solution was refluxed for 1 hour, and it was poured into a glass beaker containing 10 g of 3% Sodium Amalgam. The reaction mixture was kept for 2 hours. The solution of sodium salt of acid was isolated by decantation. After being acidified with hydrochloric acid, precipitate **4** was filtered and recrystallized from ethanol.

2.2.2. Synthesis of 2H-chromene-3-carbonyl chloride **5**.

1 g of chroman-3-carboxylic acid **4**, 1 mL of thionyl chloride, and 10 mL of benzene were refluxed for 1 hour. The 2*H*-chromene-3-carbonyl chloride **5** was isolated by vacuum distillation and used without further purification.

2.2.3. Synthesis of N-[5-(4-fluorobenzyl)-1,3-thiazol-2-yl]chroman-3-carboxamide **7**.

To a solution of 2.08 g (0.01 mol) of 5-(4-fluorobenzyl)thiazol-2-ylamine **6** and 1.5 mL of triethylamine in 15 mL of dioxane was added a solution of 1.97 g (0.01 mol) of chromane-3-carbonyl chloride in 20 mL of dioxane at room temperature. After 30 min, the reaction

mixture was poured into 100 ml of water. The resulting precipitate **7** was filtered and recrystallized from a 1:1 mixture of alcohol and DMFA.

The synthesized compound **7** is a light yellow crystalline substance, soluble in DMFA, DMSO, acetic acid, moderately soluble in cold ethanol, insoluble in water and non-polar organic solvents. Melting point 181-182°C, yield 78%.

^{1}H NMR (400 MHz, DMSO d_6) δ, ppm: 2.71-2.92 (m, 2H (4H-chromane)); 3.97 (t, 2H, *J* = 8.7 Hz (2H-chromane)); 4.02 (s, 2H CH_2); 4.32 (m, 1H (3H-chromane)); 6.7 (d, 1H, *J* = 8.0 Hz (8H-chromane)); 6.8 (t, 1H, *J* = 8.0 Hz (7H-chromane)); 6.99-7.06 (m, 4H C_6H_4F); 7.12 (s, 1H (1H-thiazole)); 7.23-7.26 (m, 2H (5,6H-chromane)); 12.21 (s, 1H, NH). Found, %: C, 65.15; H, 4.68; N, 7.56. Anal. Calcd. for $C_{20}H_{17}FN_2O_2S$, %: C, 65.20; H, 4.65; N, 7.60.

2.3. Prediction of ADME-Tox and metabolic pathways.

The pharmacokinetic properties (absorption, distribution, metabolism, excretion) and toxicity parameters for compound **7** were determined in order to estimate the perspective of using the title compounds in the process of drug development. The pkCSM [13], Swiss ADME [14], Protox_II [15], and OSIRIS methods [16] were used. The ligand-based target prediction based on 2D and 3D similarity methods [17] used web resources The SwissTargetPrediction [18]. Metabolic pathways were predicted by using [19, 20].

3. Results and Discussion

In this article, we report the synthesis antitumor activity of *N*-[5-(4-fluorobenzyl)-1,3-thiazol-2-yl]chroman-3-carboxamide **7** and analysis of future perspectives of this compound as a potential chemotherapeutic agent. Compound **7** was synthesised according to Scheme 1.

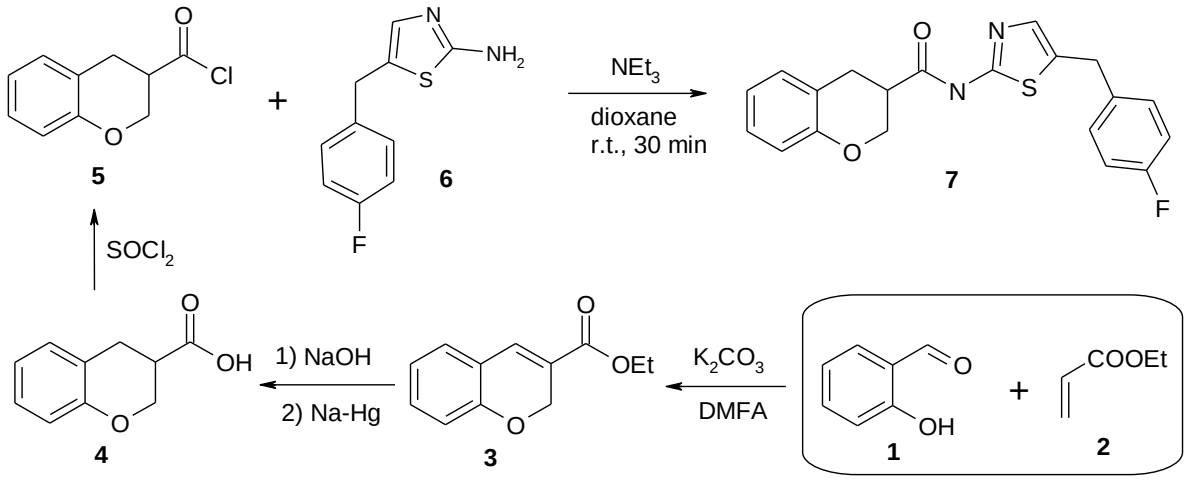

Scheme 1. Reaction pathway of synthesis of *N*-[5-(4-fluorobenzyl)-1,3-thiazol-2-yl]chroman-3-carboxamide **7**.

Salicylic aldehyde 1 was reacted with ethyl acrylate 2 under Baylis-Hilman reaction [21-23] conditions to give chromene derivative 3. The sodium salt of the acid was recovered by hydrolysis of ester 3 using sodium amalgam [24]. Acid 4 was converted to the corresponding acylchloride 5, which, by the reaction with 5-(4-fluorobenzyl)thiazol-2-ylamine 6 [25], gave the target product *N*-[5-(4-fluorobenzyl)-1,3-thiazol-2-yl]chroman-3-carboxamide 7 with yield 78%. The physicochemical and spectral characteristics of intermediates 3-6 are consistent with the literature data [23-25].

The synthesized compound 7 is a light yellow crystalline substance, soluble in DMFA, DMSO, acetic acid, moderately soluble in cold ethanol, insoluble in water and non-polar organic solvents.

3.1. In silico-target prediction.

To investigate the potential mode of action of *N*-[5-(4-fluorobenzyl)-1,3-thiazol-2-yl]chroman-3-carboxamide **7** Swiss Target Prediction software was used which showed promising affinity for a variety of enzymes, including kinases, which are targets of anticancer drugs, as well as Voltage-gated sodium channels (VGSCs) [26, 27] and G-protein-coupled receptors (GPCRs) implicated in cancer cell invasion and metastasis [28]. The top 15 targets are illustrated in Figure 2a.

The potential of compound **7** as a kinase inhibitor is also predicted by the Molinspiration Cheminformatics resource [29] (bioactivity score 0.04), Figure 2b. Protein kinases are important targets for anticancer agents [30-32].

The bioavailability of investigated compound **7** is illustrated in Figure 2c. The pink area represents the optimal range for each property, such as lipophilicity: LOGP between −0.7 and +5.0; size: MW between 150 and 500 g/mol; polarity: TPSA between 20 and 130 $Å^2$; solubility: log S not higher than 6; a fraction of sp3 of the hybridized carbon atom (INSATU): not less than 0.25; and flexibility: no more than 9 rotatable bonds. According to the bioavailability radar, compound **7** was predicted to be orally bioavailable. However, there is a slight deviation in the INSATU parameter.

The amide **7** did not violate any of the drug-likeness parameters, including Lipinski [33], Muegge [34], Ghose [35], Veber [36], and Egan [37] rules, and is not a PAINS [38] and Brenk [39] compound. According to the GSK 4/400 rule (Higher Risks of Toxicity if Log P>4 and MW>400) [40], no toxicity risks are expected for compound **7**, but according to the Pfizer 3/75 rule (lower toxicity when c Log P<3 and TPSA>75 $Å^2$) [41], the Log P value is not optimal.

The value of intestinal absorption (human) is 81.59%. The percentage of absorption (%Abs) is calculated using the known formula [42]:

$$\%Abs = 109 - 0345 * TPSA \qquad (1)$$

Compound 7 was predicted to have good skin (log Kp = -2.818), BBB (log BB = 0.094), and CNS (log PS = -1.965) permeabilities.

The BOILED-Egg Plot illustrates the ability to passively absorb in the gastrointestinal tract (HIA) and penetrate the blood-brain barrier (BBB). The white area indicates a high probability of passive absorption through the gastrointestinal tract, and the yellow area indicates a high probability of penetration into the brain. Additionally, points are colored blue if predicted to be actively effluxed by P-glycoprotein (PGP+) and red if predicted to be non-substrate of P-gp (PGP-).

According to the BOILED egg diagram (Figure 2d), a high probability of passive absorption of the gastrointestinal tract was predicted for compound **7**. It also suggests that compound **7** does not cross the blood-brain barrier (BBB) and has limited central adverse effects. Investigated amide **7** can be actively effluxed by P-glycoprotein. Reference compounds (Dasatinib, Gefitinib, 5-fluorouracil (5-FU), Curcumin, and Cisplatin) are not substrates of P-gp.

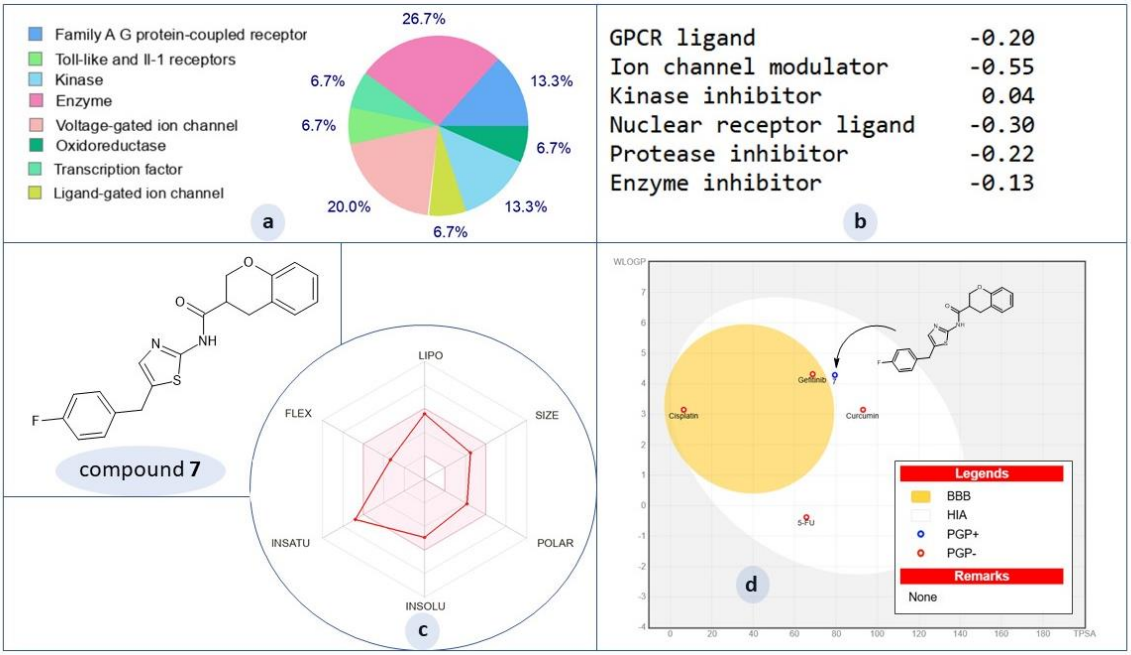

Figure 2. (a) Top 15 targets of compound **7** as predicted using SwissTarget; **(b)** Bioactivity score according to molinspiration cheminformatics; **(c)** Oral bioavailability radar; **(d)** BOILED-Egg plot.

3.2. Anticancer activity.

As already mentioned, both 2-aminothiazole and chromane derivatives have the antitumor potential [1, 11]. Taking this fact into account, *N*-1,3-thiazol-2-yl]chroman-3-carboxamide **7** was investigated for its antitumor activity. The anticancer activity of compound **7** was initially tested according to the National Cancer Institute (NCI) Developmental Therapeutic Program [www.dtp.nci.nih.gov]. The assays were performed in accordance with the NCI protocol [43–46] against 60 human tumor cell lines derived from nine types of human cancers (leukemia, non-small cell lung cancer, colon cancer, central nervous system cancer, melanoma, ovarian cancer, renal cancer, prostate cancer, and breast cancer cell lines). The results of the screening are shown in Figure 3.

As can be seen from Figure 3, compound **7** showed high antitumor activity with GP values of 67.75 – -56.28% against the tested range of cancer cells. The average GP value was 13.14%. In particular, an excellent cytotoxic effect was observed against the lines MDA-MB-435 (Melanoma) GP = -56.28%, OVCAR-3 (Ovarian Cancer) GP = -47.79%, and SF-295 (CNS Cancer) GP = -46.64%. Also compound **7** exhibited a significant cytotoxic effect on RXF 393 (Renal Cancer) GP = -34.32%, NCI-H522 (Non-Small Cell Lung Cancer) GP = -19.59%, OVCAR-4 (Ovarian Cancer) GP = -17.63%, SF-539 (CNS Cancer) GP = -17.31%, A498 (Renal Cancer) GP = -14.68%, HT29 (Colon Cancer) GP = -12.59% та NCI/ADR-RES (Ovarian Cancer) GP = -10.72% cell lines.

The protocol of the antitumor activity study is presented in Table 1 and Figure 4. The results of tested compound **7** were given by three response parameters (GI_{50}, TGI, and LC_{50}) for each cell line from the concentration of percentage growth inhibition on nine cancer diseases. The GI_{50} parameter (growth inhibitory activity) is the concentration of the compound that causes a 50% decrease in net cell growth. The TGI value (cytostatic activity) is the concentration of the compound that results in total growth inhibition. The LC_{50} value (cytotoxic activity) corresponds to the concentration of the compound that causes a net 50% loss of initial cells at the end of the 48-hour incubation period.

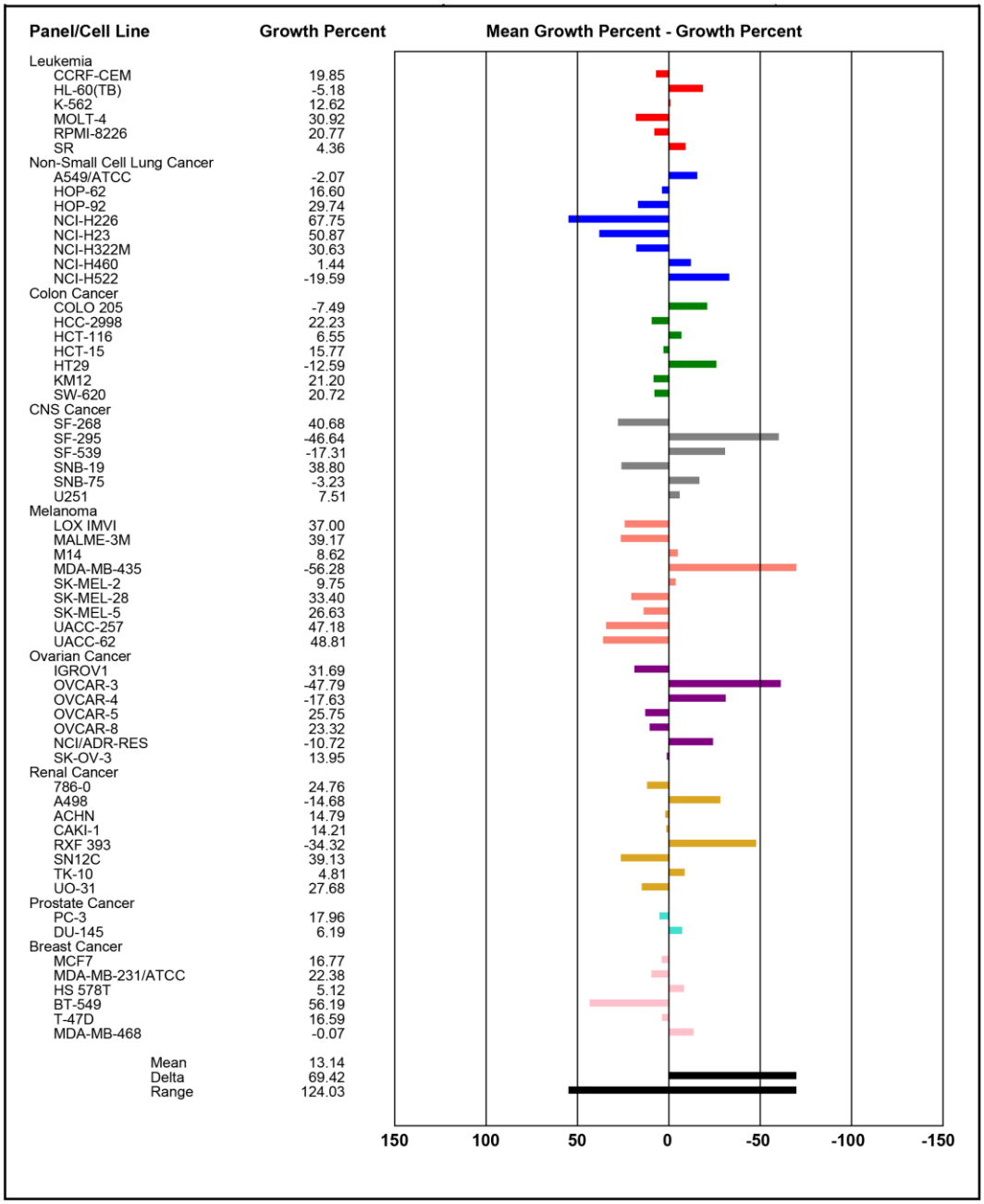

Figure 3. Sixty human tumor cell lines' anticancer screening data at single dose assay.

Table 1. NCI DTP *in vitro* testing results of compound **7** at five-dose assay (10^{-4}-10^{-8}M).

Disease	Cell line	GI_{50}, μM	TGI, μM	LC_{50}, μM	Disease	Cell line	GI_{50}, μM	TGI, μM	LC_{50}, μM
Leukemia	CCRF-CEM	0.255	>100	>100	**Ovarian cancer**	IGROV1	0.719	>100	>100
	HL-60(TB)	0.194	0.631	>100		OVCAR-3	0.218	0.636	4.36
	K-562	0.0616	>100	>100		OVCAR-4	1.600	-	>100
	MOLT-4	0.745	>100	>100		OVCAR-5	0.684	>100	>100
	RPMI-8226	0.326	2.22	>100		OVCAR-8	0.413	>100	>100
	SR	0.0384	>100	>100		NCI/ADR-RES	0.317	>100	>100
						SK-OV-3	0.435	>100	>100
Non-small cell lung cancer	A549/ATCC	0.326	3.55	>100	**Melanoma**	LOX IMVI	0.770	>100	>100
	EKVX	-	-	-		MALME-3M	2.05	>100	>100
	HOP-62	0.430	4.42	>100		M14	0.240	>100	>100
	HOP-92	0.130	2.70	>100		MDA-MB-435	0.0379	0.211	-
	NCI-H226	23.3	>100	>100		SK-MEL-2	0.245	0.941	>100

Disease	Cell line	GI_{50}, μM	TGI, μM	LC_{50}, μM	Disease	Cell line	GI_{50}, μM	TGI, μM	LC_{50}, μM
	NCI-H23	0.482	>100	>100		SK-MEL-28	0.823	>100	>100
	NCI-H322M	2.48	>100	>100		SK-MEL-5	0.333	>100	>100
	NCI-H460	0.318	1.17	>100		UACC-257	0.692	>100	>100
	NCI-H522	0.136	0.591	>100		UACC-62	0.417	>100	>100
Colon cancer	COLO 205	0.307	1.06	>100	**Renal cancer**	786-0	0.910	>100	>100
	HCC-2998	0.523	>100	>100		A498	0.200	0.772	>100
	HCT-116	0.406	>100	>100		ACHN	1.51	>100	>100
	HCT-15	0.191	>100	>100		CAKI-1	0.467	>100	>100
	HT29	0.251	1.21	>100		RXF 393	0.267	0.916	>100
	KM12	0.141	15.2	>100		SN12C	0.751	>100	>100
	SW-620	0.272	>100	>100		TK-10	0.517	3.17	>100
						UO-31	1.02	>100	>100
CNS cancer	SF-268	0.897	>100	>100	**Breast cancer**	MCF7	0.0828	>100	>100
	SF-295	0.223	1.62	>100		MDA-MB-231/ATCC	0.381	5.02	>100
	SF-539	0.215	0.569	58.4					
	SNB-19	2.42	>100	>100		HS 578T	0.325	4.32	>100
	SNB-75	0.282	3.87	>100		BT-549	>100	>100	>100
	U251	0.345	1.77	>100		T-47D	0.557	8.54	>100
Prostate cancer	PC-3	0.277	>100	>100		MDA-MB-468	0.316	>100	>100
	DU-145	0.368	25.4	>100					

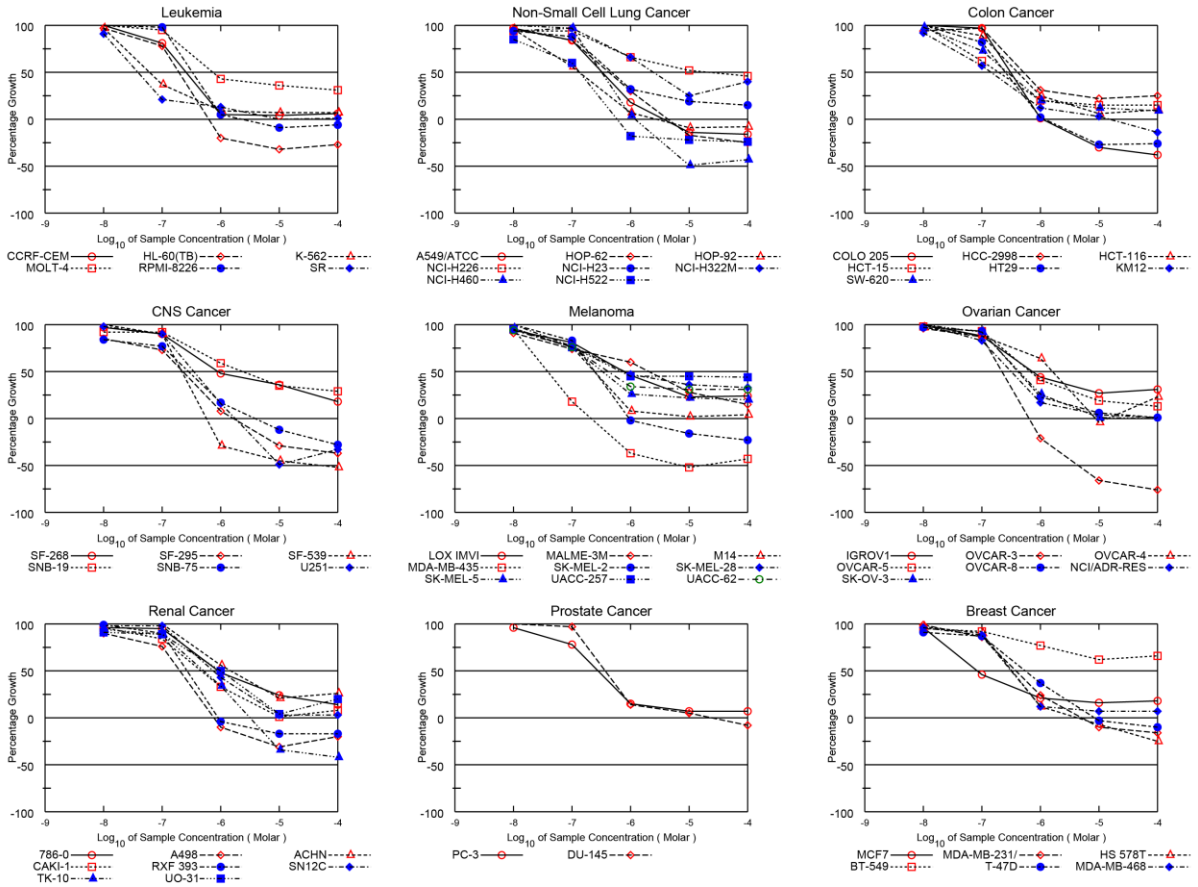

Figure 4. Dose-response curves (% growth versus sample concentration at NCI fixed protocol, μM) were obtained from the NCI's *in vitro* disease-oriented human tumor cells line of compound **7** on nine cancer diseases.

The title compound **7** exhibited remarkable anticancer activity against all the tested cell lines. The most sensitive to the compound was Leukemia and Prostate Cancer cell lines, and

the compound significantly inhibited the growth of Melanoma, Colon Cancer, Renal Cancer, and Non-Small Cell Lung Cancer tumor cells. The effectiveness of inhibition of tumor cell growth of the claimed compound exceeds that of the classical anticancer drugs gefitinib, 5-fluorouracil, cisplatin, and curcumin. The antitumor effect of the tested compound **7** against K-562 (Leukemia), SR (Leukemia), MDA-MB-435 (Melanoma), and MCF7 (Breast Cancer) cell lines was observed in nano concentrations.

To interpret the results of the antitumor activity screening, we calculated the selectivity index (SI) at the GI_{50} level of compound **7**, which is equal to the ratio of the average MG-MID activity (μM) for all cell lines to the average value of the corresponding subpanel of cancer. The value of the SI index in the range of 3-6 refers to moderate selectivity. A value of SI > 6 indicates high selectivity for the corresponding cell line. Suppose SI < 3, the antitumor effect is considered non-selective [47]. In this context, the active compound **7** demonstrates moderate selectivity against the Leukemia cell line (Table 2).

However, high selectivity was observed for individual cell lines: K-562 (Leukemia) SI = 22.24 (full cancer panel), SI = 5. 422 (Leukemia panel); SR (Leukemia) SI = 35.68 (full cancer panel), SI = 8.698 (Leukemia panel); MDA-MB-435 (Melanoma) SI = 36.15 (full cancer panel), SI = 16.20 (Melanoma panel) and MCF7 (Breast Cancer) SI = 16.55 (full cancer panel), SI = 50.92 (Breast Cancer panel).

We also evaluated the metabolic pathway of compound **7** mediated by Cytochrome P450. It was found that the main pathways are aromatic hydroxylation of the fused benzene ring, hydroxylation of aromatic carbon, hydroxylation of non-terminal aliphatic carbon adjacent to the aromatic ring, alpha-hydroxylation of carbonyl group, *N*-hydroxylation of secondary arylamide, and dehydration of the pyran cycle. Formation of a potentially toxic metabolite such as M11 [48] is not expected (Figure 5).

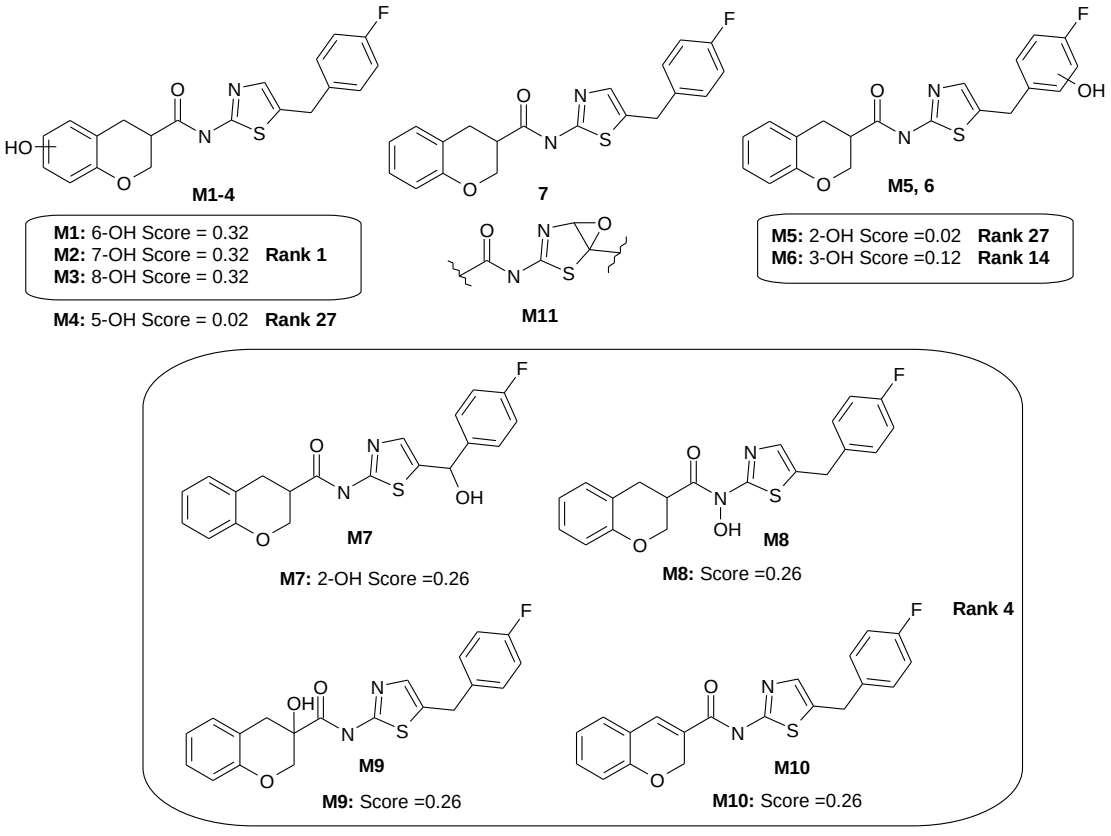

Figure 5. Predicted pathway of title compound **7**.

Table 2. The average inhibitory concentration of tumor cell growth (GI_{50}, μM) of compound **7** in comparison with known anticancer agents - gefitinib, 5-fluorouracil, cisplatin, curcumin, and selectivity index (SI) at the GI_{50} level of compound **7**.

Compound 7 and reference drugs	Cancer panel / GI_{50} (C, μM)									
	L*	NSCLC	ColC	CNSC	M	OV	RC	PC	BC	MG-MID
Compound **7**	0.334	2.111	0.799	0.884	0.614	2.136	0.838	0.395	4.216	1.370
SI** of cpd **7**	4.101	0.649	1.715	1.550	2.231	0.641	1.635	3.468	0.325	-
Gefitinib	3.54	7.81	7.02	8.14	5.28	6.63	2.67	1.65	7.81	3.24
5-Fluorouracil	15.1	>100	8.4	72.1	70.6	61.4	45.6	22.7	76.4	52.5
Cisplatin	6.3	9.4	21.0	4.7	8.5	6.3	10.2	5.6	13.3	9.48
Curcumin	3.7	9.2	4.7	5.8	7.1	8.9	10.2	11.2	5.9	7.41

*L – Leukemia, NSCLC – Non-small cell lung Cancer, ColC – Colon Cancer, CNSC – CNS Cancer, M – Melanoma, OV– Ovarian Cancer, RC – Renal Cancer, PC – Prostate Cancer, BC – Breast Cancer, MG-MID – the average inhibitory concentration for the full panel of cancer cell types tested; **SI – Selectivity index at the GI_{50} level.

The calculations performed using OSIRIS Property Explorer for compound **7** do not expect mutagenic, tumourigenic, irritant, or toxic reproductive effects. According to Protox_II online resource: Predicted LD_{50} = 300mg/kg (Toxicity Class: 3).

4. Conclusions

N-[5-(4-fluorobenzyl)-1,3-thiazol-2-yl]chroman-3-carboxamide was synthesized by the reaction of chroman-3-carbonyl chloride with 5-(4-fluorobenzyl)thiazol-2-ylamine. This compound complies with Lipinski, Muegge, Ghose, Veber, and Egan rules. It displays favorable pharmacokinetics indices, a good ADME-Tox profile, and a remarkable metabolic pathway, which does not involve the formation of toxic metabolites. Title compound is useful as a promising scaffold in the designing of novel active anticancer candidates.

Funding

This work was supported by the Ministry of Health of Ukraine (Grant 0124U001313) and the Simons Foundation (Award No 1290588).

Acknowledgments

We are grateful to the Drug Synthesis and Chemistry Branch, National Cancer Institute, Bethesda, MD, USA, for the *in vitro* evaluation of the anticancer activity.

Conflicts of Interest

The authors declare no conflict of interest.

References

1. Wan, Y.; Long, J.; Gao, H.; Tang, Z. 2-Aminothiazole: A privileged scaffold for the discovery of anti-cancer agents. *Eur J Med Chem.* **2021**, *210*, 112953, https://doi.org/10.1016/j.ejmech.2020.112953.
2. Farouk Elsadek, M.; Mohamed Ahmed, B.; Fawzi Farahat, M. An Overview on Synthetic 2-Aminothiazole-Based Compounds Associated with Four Biological Activities. *Molecules* **2021**, *26*, 1449, https://doi.org/10.3390/molecules26051449.
3. Younes, A.H.; Mustafa, Y.F. Plant-Derived Coumarins: A Narrative Review of Their Structural and Biomedical Diversity. *Chem Biodivers* **2024**, *21*, e202400344, https://doi.org/10.1002/cbdv.202400344.
4. Kamboj, S.; Singh, R. Chromanone-A Prerogative Therapeutic Scaffold: An Overview. *Arab J Sci Eng* **2022**, *47*, 75-111, https://doi.org/10.1007/s13369-021-05858-3.

5. Dash, A.K.; Kumar, D. The Role of Chromenes in Drug Discovery and Development. Dash, A.K., Kumar, D., Eds.; Bentham Science Publishers: **2023**; https://doi.org/10.2174/9789815124330123010101.
6. Flores-Morales, V.; Villasana-Ruíz, A.P.; Garza-Veloz, I.; González-Delgado, S.; Martinez-Fierro, M.L. Therapeutic Effects of Coumarins with Different Substitution Patterns. *Molecules* **2023**, *28*, 2413, https://doi.org/10.3390/molecules28052413.
7. Reis, J.; Gaspar, A.; Milhazes, N.; Borges, F. Chromone as a Privileged Scaffold in Drug Discovery: Recent Advances. *J Med Chem* **2017**, *60*, 7941-7957, https://doi.org/10.1021/acs.jmedchem.6b01720.
8. Costa, M.; Dias, T.A.; Brito, A.; Proença, F. Biological importance of structurally diversified chromenes. *Eur J Med Chem* **2016**, *123*, 487-507, https://doi.org/10.1016/j.ejmech.2016.07.057.
9. Raj, V.; Lee, J. 2H/4H-Chromenes-A Versatile Biologically Attractive Scaffold. *Front Chem* **2020**, *8*, 623, https://doi.org/10.3389/fchem.2020.00623.
10. Chaudhary, A.; Singh, K.; Verma, N.; Kumar, S.; Kumar, D.; Sharma, P.P. Chromenes - A Novel Class of Heterocyclic Compounds: Recent Advancements and Future Directions. *Mini Rev Med Chem* **2022**, *22*, 2736-2751, https://doi.org/10.2174/1389557522666220331161636.
11. Grover, P.; Gulati, H.K.; Jasha Momo H. Anál; Mukherjee D. Chromenes as Anticancer Agents. In The Role of Chromenes in Drug Discovery and Development. Dash, A.K., Kumar, D., Eds.; Bentham Science Publishers: **2023**; pp. 190-214, https://doi.org/10.2174/9789815124330123010011.
12. Sharon, K.N.; Padmaja, P.; Reddy, N. A Brief Review on the Synthesis of 4H-Chromene-Embedded Heterocycles. *ChemistrySelect* **2024**, *9*, e202400565, https://doi.org/10.1002/slct.202400565.
13. Pires, D.E.; Blundell, T.L.; Ascher, D.B. pkCSM: Predicting Small-Molecule Pharmacokinetic and Toxicity Properties Using Graph-Based Signatures. *J Med Chem* **2015**, *58*, 4066-4072, https://doi.org/10.1021/acs.jmedchem.5b00104.
14. Daina, A.; Michielin, O.; Zoete, V. SwissADME: a free web tool to evaluate pharmacokinetics, drug-likeness and medicinal chemistry friendliness of small molecules. *Sci Rep* **2017**, *7*, 42717, https://doi.org/10.1038/srep42717.
15. Banerjee, P.; Eckert, A.O.; Schrey, A.K.; Preissner, R. ProTox-II: a webserver for the prediction of toxicity of chemicals. *Nucleic Acids Res* **2018**, *46*, W257-W263, https://doi.org/10.1093/nar/gky318.
16. Sander, T.; Freyss, J.; von Korff, M.; Reich, J.R.; Rufener, C. OSIRIS, an entirely in-house developed drug discovery informatics system. *J Chem Inf Model* **2009**, *49*, 232-246, https://doi.org/10.1021/ci800305f.
17. Downs, G.M.; Willett, P. Similarity Searching in Databases of Chemical Structures. In Reviews in Computational Chemistry; Reviews in Computational Chemistry; Lipkowitz, K.B., Boyd, D.B., Eds.; John Wiley & Sons: **1996**; pp. 1-66, https://doi.org/10.1002/9780470125847.ch1.
18. Daina, A.; Michielin, O.; Zoete, V. SwissTargetPrediction: updated data and new features for efficient prediction of protein targets of small molecules. *Nucleic Acids Res* **2019**, *47*, W357-W364, https://doi.org/10.1093/nar/gkz382.
19. de Bruyn Kops, C.; Šícho, M.; Mazzolari, A.; Kirchmair, J. GLORYx: Prediction of the Metabolites Resulting from Phase 1 and Phase 2 Biotransformations of Xenobiotics. *Chem Res Toxicol* **2021**, *34*, 286-299, https://doi.org/10.1021/acs.chemrestox.0c00224.
20. Stork, C.; Embruch, G.; Šícho, M.; de Bruyn Kops, C.; Chen, Y.; Svozil, D.; Kirchmair, J. NERDD: a web portal providing access to in silico tools for drug discovery. *Bioinformatics* **2020**, *36*, 1291-1292, https://doi.org/10.1093/bioinformatics/btz695.
21. Basavaiah, D.; Rao, A.J.; Satyanarayana T. Recent advances in the Baylis-Hillman reaction and applications. *Chem Rev* **2003**, *103*, 811-892, https://doi.org/10.1021/cr010043d.
22. Basavaiah, D.; Veeraraghavaiah G. The Baylis-Hillman reaction: a novel concept for creativity in chemistry. *Chem Soc Rev* **2012**, *41*, 68-78, https://doi.org/10.1039/c1cs15174f.
23. Pan, J.; Yin, Y.; Zhao, L.; Feng Y. Discovery of (S)-6-methoxy-chroman-3-carboxylic acid (4-pyridin-4-yl-phenyl)-amide as potent and isoform selective ROCK2 inhibitors. *Bioorg Med Chem* **2019**, *27*, 1382-1390, https://doi.org/10.1016/j.bmc.2019.02.047.
24. Babcock Jr, S.H.; Lankelma, H.P.; Vopicka, E. Sodium Amalgam. In Inorganic Syntheses; Booth, H.S., Ed.; **1939**; pp. 10-11, https://doi.org/10.1002/9780470132326.ch4.
25. Pokhodylo, N.; Finiuk, N.; Klyuchivska, O.; Stoika, R.; Matiychuk, V.; Obushak, M. Bioisosteric replacement of 1H-1,2,3-triazole with 1H-tetrazole ring enhances anti-leukemic activity of (5-benzylthiazol-2-yl)benzamides. *Eur J Med Chem* **2023**, *250*, 115126, https://doi.org/10.1016/j.ejmech.2023.115126.

26. Sakellakis, M.; Yoon, S.M.; Jashan Reet; Chalkias, A. Novel insights into voltage-gated ion channels: Translational breakthroughs in medical oncology. *Channels* **2024**, *18*, 2297605, https://doi.org/10.1080/19336950.2023.2297605.
27. Angus, M.; Ruben, P. Voltage gated sodium channels in cancer and their potential mechanisms of action. *Channels* **2019**, *13*, 400-409, https://doi.org/10.1080/19336950.2019.1666455.
28. Chaudhary, P.K.; Kim, S. An Insight into GPCR and G-Proteins as Cancer Drivers. *Cells* **2021**, *10*, 3288, https://doi.org/10.3390/cells10123288.
29. Molinspiration Cheminformatics. Calculation of Molecular Properties and Bioactivity Score. Available online: https://molinspiration.com/cgi/properties (accessed on 1 December **2024**).
30. Bhullar, K.S.; Lagarón, N.O.; McGowan, E.M.; Parmar, I.; Jha, A.; Hubbard, B.P.; Rupasinghe, H.P.V. Kinase-targeted cancer therapies: progress, challenges and future directions. *Mol Cancer* **2018**, *17*, 48, https://doi.org/10.1186/s12943-018-0804-2.
31. Singha, M.; Pu, L.; Srivastava, G.; Ni, X.; Stanfield, B.A.; Uche, I.K.; Rider, P.J.F.; Kousoulas, K.G.; Ramanujam, J.; Brylinski, M. Unlocking the Potential of Kinase Targets in Cancer: Insights from CancerOmicsNet, an AI-Driven Approach to Drug Response Prediction in Cancer. *Cancers* **2023**, *15*, 4050, https://doi.org/10.3390/cancers15164050.
32. Li, J.; Gong, C.; Zhou, H.; Liu, J.; Xia, X.; Ha, W.; Jiang, Y.; Liu, Q.; Xiong, H. Kinase Inhibitors and Kinase-Targeted Cancer Therapies: Recent Advances and Future Perspectives. *Int J Mol Sci* **2024**, *25*, 5489, https://doi.org/10.3390/ijms25105489.
33. Lipinski, C.A.; Lombardo, F.; Dominy, B.W.; Feeney, P.J. Experimental and computational approaches to estimate solubility and permeability in drug discovery and development settings. *Advanced Drug Delivery Reviews* **1997**, *23*, 3-25, https://doi.org/10.1016/S0169-409X(96)00423-1.
34. Muegge, I.; Heald, S.L.; Brittelli, D. Simple selection criteria for drug-like chemical matter. *J Med Chem* **2001**, *44*, 1841-1846, https://doi.org/10.1021/jm015507e.
35. Ghose, A.K.; Viswanadhan, V.N.; Wendoloski, J.J. A knowledge-based approach in designing combinatorial or medicinal chemistry libraries for drug discovery. 1. A qualitative and quantitative characterization of known drug databases. *J Comb Chem* **1999**, *1*, 55-68, https://doi.org/10.1021/cc9800071.
36. Veber, D.F.; Johnson, S.R.; Cheng, H.Y.; Smith, B.R.; Ward, K.W.; Kopple, K.D. Molecular properties that influence the oral bioavailability of drug candidates. *J Med Chem* **2002**, *45*, 2615-23, https://doi.org/10.1021/jm020017n.
37. Egan, W.J.; Merz, K.M.Jr; Baldwin, J.J. Prediction of drug absorption using multivariate statistics. *J Med Chem* **2000**, *43*, 3867-3877, https://doi.org/10.1021/jm000292e.
38. Baell, J.B.; Holloway, G.A. New substructure filters for removal of pan assay interference compounds (PAINS) from screening libraries and for their exclusion in bioassays. *J Med Chem* **2010**, *53*, 2719-40, https://doi.org/10.1021/jm901137j.
39. Brenk, R.; Schipani, A.; James, D.; Krasowski, A.; Gilbert, I.H.; Frearson, J.; Wyatt, P.G. Lessons learnt from assembling screening libraries for drug discovery for neglected diseases. *ChemMedChem* **2008**, *3*, 435-444, https://doi.org/10.1002/cmdc.200700139.
40. Gleeson, M.P. Generation of a set of simple, interpretable ADMET rules of thumb. *J Med Chem* **2008**, *51*, 817-834, https://doi.org/10.1021/jm701122q.
41. Hughes, J.D.; Blagg, J.; Price, D.A.; Bailey, S.; Decrescenzo, G.A.; Devraj, R.V.; Ellsworth, E.; Fobian, Y.M.; Gibbs, M.E.; Gilles, R.W.; Greene, N.; Huang, E.; Krieger-Burke, T.; Loesel, J.; Wager, T.; Whiteley, L.; Zhang, Y. Physiochemical drug properties associated with in vivo toxicological outcomes. *Bioorg Med Chem Lett* **2008**, *18*, 4872-4875, https://doi.org/10.1016/j.bmcl.2008.07.071.
42. Zhao, Y.H.; Abraham, M.H.; Le, J.; Hersey, A.; Luscombe, C.N.; Beck. G.; Sherborne, B.; Cooper, I. Rate-limited steps of human oral absorption and QSAR studies. *Pharm Res* **2002**, *19*, 1446-1457, https://doi.org/10.1023/a:1020444330011.
43. Monks, A.; Scudiero, D.; Skehan, P.; Shoemaker, R.; Paull, K.; Vistica, D.; Hose, C.; Langley, J.; Cronise, P.; Vaigro-Wolff, A.; Gray-Goodrich, M.; Campbell, H.; Joseph, Mayo; Boyd, M. Feasibility of a High-Flux Anticancer Drug Screen Using a Diverse Panel of Cultured Human Tumor Cell Lines. *J Nat Cancer Inst* **1991**, *83*, 757-766, https://doi.org/10.1093/jnci/83.11.757.
44. Boyd, M.R.; Paull, K.D. Some practical considerations and applications of the national cancer institute *in vitro* anticancer drug discovery screen. *Drug Dev Res* **1995**, *34*, 91-109, https://doi.org/10.1002/ddr.430340203.

45. Boyd, M.R. The NCI *In vitro* Anticancer Drug Discovery Screen. In Anticancer Drug Development Guide: Preclinical Screening, Clinical Trials, and Approval, Teicher, B.A., Ed.; Humana Press: Totowa, NJ, **1997**; pp. 23-42, https://link.springer.com/chapter/10.1007/978-1-4615-8152-9_2.
46. Selby, M.; Delosh, R.; Laudeman, J.; Ogle, C.; Reinhart, R.; Silvers, T.; Lawrence, S.; Kinders, R.; Parchment, R.; Teicher, B.A.; Evans, D.M. 3D Models of the NCI60 Cell Lines for Screening Oncology Compounds. *SLAS Discov* **2017**, *22*, 473-483, https://doi.org/10.1177/2472555217697434.
47. Rostom, S.A. Synthesis and *in vitro* antitumor evaluation of some indeno[1,2-c]pyrazol(in)es substituted with sulfonamide, sulfonylurea(-thiourea) pharmacophores, and some derived thiazole ring systems. *Bioorg Med Chem* **2006**, *14*, 6475-6485, https://doi.org/10.1016/j.bmc.2006.06.020.
48. Jaladanki, C.K.; Khatun, S.; Gohlke, H.; Bharatam, P.V. Reactive Metabolites from Thiazole-Containing Drugs: Quantum Chemical Insights into Biotransformation and Toxicity. *Chem Res Toxicol* **2021**, *34*, 1503-1517, https://doi.org/10.1021/acs.chemrestox.0c00450.